Original Research

Caveolin-1 expression during the progression of pulmonary hypertension

Jing Huang[1], John H Wolk[2], Michael H Gewitz[1] and Rajamma Mathew[1,3]

[1]Section of Pediatric Cardiology, Maria Fareri Children's Hospital, New York Medical College; [2]Department of Pathology; [3]Department of Physiology, New York Medical College, Valhalla, NY 10595, USA
Corresponding author: Rajamma Mathew. Email: rajamma_mathew@NYMC.edu

Abstract

Caveolin-1 plays a pivotal role in maintaining vascular health. Progressive loss of endothelial caveolin-1 and activation of proliferative and anti-apoptotic pathways occur before the onset of monocrotaline (MCT)-induced pulmonary hypertension (PH), and the rescue of endothelial caveolin-1 attenuates PH. Recently, we reported endothelial caveolin-1 loss associated with enhanced expression of caveolin-1 in smooth muscle cells (SMC) with subsequent neointima formation in human PH. To examine whether the loss of endothelial caveolin-1 followed by an enhanced expression in SMC is a sequential event in the progression of PH, we studied rats at two and four weeks post-MCT. Right ventricular (RV) systolic pressure, RV hypertrophy, pulmonary vascular histology, and the expression of caveolin-1 and endothelial membrane proteins (platelet/endothelial cell adhesion molecule-1 [PECAM-1], both α and β subunits of soluble guanylate cyclase [sGC]), von Willebrand factor (vWF), smooth muscle α-actin, proliferative and anti-apoptotic factors (PY-STAT3 and Bcl-xL) and matrix metalloproteinase (MMP) 2 in the lungs were examined. PH was accompanied by a progressive loss of endothelial caveolin-1, activation of PY-STAT3, increased Bcl-xL expression and vascular remodeling at two and four weeks post-MCT. Loss of PECAM-1 and sGC (both subunits) paralleled that of caveolin-1, whereas vWF was well preserved at two weeks post-MCT. At four weeks post-MCT, 29% of the arteries showed a loss of vWF in addition to endothelial caveolin-1, and 70% of these arteries exhibited enhanced expression of caveolin-1 in SMC; and there was increased expression and activity of MMP2. In conclusion, MCT-induced endothelial injury disrupts endothelial cell membrane with a progressive loss of endothelial caveolin-1, and the activation of proliferative and antiapoptotic pathways leading to PH. Subsequent extensive endothelial cell damage results in enhanced expression of caveolin-1 in SMC. In addition, there is a progressive increase in MMP2 expression and activity. These alterations may further facilitate cell proliferation, matrix degradation and cell migration, thus contributing to the progression of the disease.

Keywords: caveolin-1, endothelial cells, pulmonary hypertension, smooth muscle cells, vWF

Experimental Biology and Medicine 2012; **237**: 956–965. DOI: 10.1258/ebm.2012.011382

Introduction

Pulmonary hypertension (PH) is a devastating disease with a high morbidity and mortality rate. Because of vague clinical symptoms, it is often difficult to make the diagnosis of PH early. Another confounding factor is that a variety of cardiopulmonary and other systemic diseases can lead to PH. By the time the diagnosis is made, the pulmonary arteries in a number of patients exhibit significant changes such as activation of proliferative and antiapoptotic factors, vascular remodeling, obstruction in the small pulmonary arteries and elevated pressure.[1–3] Endothelial dysfunction is the major and possibly the initial underlying defect in PH, and impaired endothelium-dependent vascular relaxation is a common feature of clinical and experimental PH.[4] The endothelial damage is progressive, and the extensive endothelial damage and/or loss leads to further cell proliferation, cell migration and neointima formation, contributing to failure of therapy and poor prognosis.[5] Since PH presents itself relatively late in the clinical setting, it is impossible to unravel the sequence of events occurring during the progression of the disease, and ultimately pulmonary vasculature becoming unresponsive to therapy. Animal models, although not considered entirely identical to human forms of PH, have been quite useful in understanding the mechanism/s of the disease process and for testing the efficacy of new drugs.

Monocrotaline (MCT), an inflammatory model of PH, has been extensively studied to understand the mechanism of PH. We have previously shown the disruption of

endothelial cell membrane, progressive loss of endothelial caveolin-1, and reciprocal activation (tyrosine phosphorylation) of a proproliferative transcription factor, signal transducer and activator of transcription 3 (PY-STAT3) and increased expression of Bcl-xL (antiapoptotic factor) to occur within 48 h of MCT injection, i.e. before the onset of PH. In addition, other endothelial proteins such as platelet/endothelial cell adhesion molecule-1 (PECAM-1), Tie2 and soluble guanylate cyclase (α and β subunits) are lost in tandem with caveolin-1, indicating a generalized endothelial cell membrane disruption.[6–8] As the disease progresses, by two weeks post-MCT, the expression of several cytosolic proteins such as HSP90, protein kinase B (also known as Akt) and inhibitory κB-α is significantly reduced. The expression of endothelial nitric oxide synthase (eNOS) is significantly increased at 48 h and one week post-MCT, possibly as a compensatory mechanism. Importantly, 48 h and one week post-MCT, there is no evidence of PH or right ventricular hypertrophy (RVH). By two weeks post-MCT, eNOS expression is reduced but not significantly lower compared with the controls. Loss of eNOS-activating molecules (HSP90 and Akt) at two weeks is accompanied by impaired endothelium-dependent vascular relaxation response, low sulfhydryl and cyclic guanosine monophosphate levels and superoxide generation indicating eNOS uncoupling. At this stage, significant pulmonary vascular remodeling, PH and RVH are evident. At three weeks post-MCT, there is a significant reduction in the expression of eNOS, and interestingly, the superoxide generation returns to normal levels.[4,7–9] Rescue of caveolin-1 inhibits the activation of proliferative pathways and attenuates MCT-induced PH. However, once the MCT-induced PH is established, most therapeutic agents fail to rescue endothelial caveolin-1 or to attenuate PH.[8]

Caveolin-1, a 22 kDa protein, is the major resident scaffolding protein constituent of caveolae, the omega-shaped invaginations (size 50–100 nm) in the plasma membrane of a variety of cells including epithelial, endothelial cells (EC), fibroblasts and smooth muscle cells (SMC). Caveolae, rich in cholesterol and sphingolipids, participate in lipid transport, membrane trafficking and function as a platform for numerous signaling molecules. Caveolin-1 directly interacts with transducing molecules including G proteins, src family of tyrosine kinases and eNOS. The interaction of different proteins with caveolin scaffolding domain leads to the inhibition of the protein function and these proteins are retained in an inactive conformation.[10–12] Caveolin-1, also known as a tumor suppressor, functions as an antiproliferative molecule; it negatively regulates proliferative pathways such as MAPK/ERK (mitogen-activated protein kinase/extracellular signal-regulated kinase), PY-STAT3, EGF (endothelial growth factor) and PDGF (platelet-derived growth factor) (reviewed in ref.[13]). Caveolin-1 also regulates cell cycle and apoptosis.[14,15] Furthermore, caveolin-1 participates in Ca^{2+} homeostasis, and in SMC, it regulates Ca^{2+} entry and enables vasoconstriction.[16] Thus, caveolin-1 plays an important role in maintaining vascular health.

We have recently reported the loss of endothelial caveolin-1 and von Willebrand factor (vWF) associated with an enhanced expression of caveolin-1 in pulmonary vascular SMC in a child who developed pulmonary arterial hypertension (PAH) two years after a complete clinical recovery from acute respiratory distress syndrome (ARDS). The major defect in ARDS is endothelial damage resulting in increased pulmonary vascular permeability. In this case, despite apparent clinical recovery from ARDS, the endothelial damage appears to have been progressive. Interestingly, enhanced expression of caveolin-1 in SMC was found only in the arteries which exhibited loss of vWF coupled with endothelial caveolin-1 loss. This was followed by neointima formation and a rapid downhill course.[5] Since vWF is stored in Weibel Palade bodies within the endothelial cells, its loss indicates extensive endothelial damage. Therefore, it is not surprising that the increased plasma levels of vWF and circulating endothelial cells are considered markers of poor prognosis in PH.[17,18] Interestingly, enhanced expression of caveolin-1 in pulmonary vascular SMC isolated from patients with idiopathic PAH has been found to be pro-proliferative, with a capacity to participate in DNA synthesis.[19]

Based on these observations, we hypothesized that the enhanced expression of caveolin-1 in SMC is a sequential event during the progression of PH and it follows extensive endothelial damage. To test our hypothesis, we examined the alterations in the expression of caveolin-1 and other endothelial cell membrane proteins PECAM-1 and sGC (α and β subunits), and vWF, smooth muscle α-actin, PY-STAT3 and Bcl-xL in the lungs of MCT-injected rats at two and four weeks. In addition, we examined the expression of matrix metalloproteinase (MMP) 2, because increased MMP2 expression has been reported in PAH; and MMP2 degrades extracellular matrix and facilitates cell proliferation and migration. Furthermore, caveolin-1 is known to inhibit MMP2 activity.[20,21] We demonstrate that the endothelial caveolin-1 loss caused by MCT-induced endothelial damage is progressive, accompanied by the activation of proliferative and antiapoptotic factors. As the disease progresses, the loss of vWF, in addition to a further loss of endothelial caveolin-1, is followed by an enhanced expression of caveolin-1 in SMC. At two and four weeks post-MCT, there is a three- to seven-fold increase in the expression of MMP2, which may facilitate further proliferation, and cell migration, thus contributing to the worsening of the disease.

Materials and methods

Animals

Male Sprague–Dawley rats weighing 170–180 g were obtained from Charles River (Wilmington, MA, USA). Rats were allowed to acclimatize in the animal facility for five days before the start of experimental protocols, and had free access to laboratory chow and water. MCT solution was freshly prepared on the day of use as previously described.[6–9] Rats received a single subcutaneous injection of MCT (60 mg/kg) and were studied at two and four weeks post-MCT. Data from control rats studied at two and four weeks in parallel with the MCT rats were pooled

for statistical analysis. Protocols were approved by the Institutional Animal Care and Use Committee, and conformed to the Guiding Principles for the Use and Care of Laboratory Animals of the American Physiological Society and the National Institutes of Health.

Chemicals and antibodies

All chemicals including MCT were bought from Sigma-Aldrich (St Louis MO, USA), except for Coomassie Brilliant Blue G-250 and Precision plus protein dual color standards, which were obtained from Bio-Rad (Hercules, CA, USA). Antibodies: caveolin-1α (sc894), PECAM-1 (sc1506) and MMP2 (sc13595) were obtained from Santa Cruz Laboratories (Santa Cruz, CA, USA), vWF (A0082) from Dako (Carpentaria, CA, USA), smooth muscle α-actin (A2547), β-actin (A5441) and MMP2 (M4065) from Sigma, PY-STAT3 (#9145) and Bcl-xL (#2764) from Cell Signaling (Beverly, MA, USA), sGC α and β subunits from Cayman Chemical Co. (Ann Arbor, MI, USA), and STAT3 (#610189) from BD Biosciences (Palo Alto, CA, USA).

Measurements of right ventricular systolic pressure

Right ventricular systolic pressure (RVSP) was measured using methods described previously.[6–9] Briefly, rats were anesthetized with an intraperitoneal injection of pentobarbital (60 mg/kg). The sedation was monitored carefully; more pentobarbital was given if rats were not completely anesthetized with the usual dose. Through an incision in the neck, the trachea was exposed and cannulated with PE240 tubing, and the rat ventilated in room air at a rate of approximately 70–80 breaths per minute with a tidal volume of 0.83 mL/100 g body weight. The chest was opened; PE50 tubing inserted into the RV and the pressure recorded on a Grass polygraph (model 7E: Grass Technologies, Quincy, MA, USA). At the end of the pressure measurements, the lungs were perfused with autoclaved normal saline to remove blood. The left lung and the heart were placed in 10% buffered formaldehyde. The right lung was quickly frozen in liquid nitrogen and stored at -80°C for protein extraction at a later date.

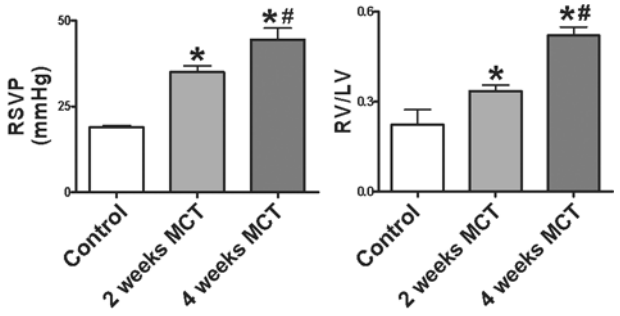

Figure 1 Right ventricular systolic pressure (RVSP) and right ventricular hypertrophy (RVH). This figure shows progressive increase in RVSP at two and four weeks post-monocrotaline (MCT). Similarly, at two and four weeks post-MCT, there is progressive RVH as assessed by the weight ratio of free wall of the right ventricle (RV) to left ventricle and the septum (LV + S). $^{*}P < 0.05$ versus controls, $^{\#}P < 0.05$ versus two weeks post-MCT ($n = 4$)

Assessment of RVH

A week later, the heart was removed from formaldehyde and the atria were trimmed. The free wall of the RV was separated from the left ventricle (LV) and the septum. The ratio of RV/LV was calculated to assess RVH.

Western blot analysis

Western blot analysis was carried out as previously described.[6–8] Briefly, the lung tissue was homogenized in a buffer containing 0.1 mol/L phosphate-buffered saline (PBS, pH 7.4), 0.5% sodium deoxycholate, 1% Igepal, 0.1% sodium dodecyl sulfate (SDS), 10 μL/mL phenylmethylsulfonic fluoride (PMSF, 10 mg dissolved in 1 ml of isopropanol), 25 μg /mL aprotinin and 25 μg/mL leupeptin. PMSF (10 μL/mL) and phosphatase Inhibitor Cocktail 1 (10 μL/mL) were added to homogenates placed on ice for 30 min, and centrifuged at 15,000 rpm for 20 min at 4°C. Protein concentrations in the supernatants were analyzed by Lowry's method using serum albumen as standard (Bio-Rad kit). Fifty or 100 μg of protein from lung supernatants were loaded and separated on a 10%

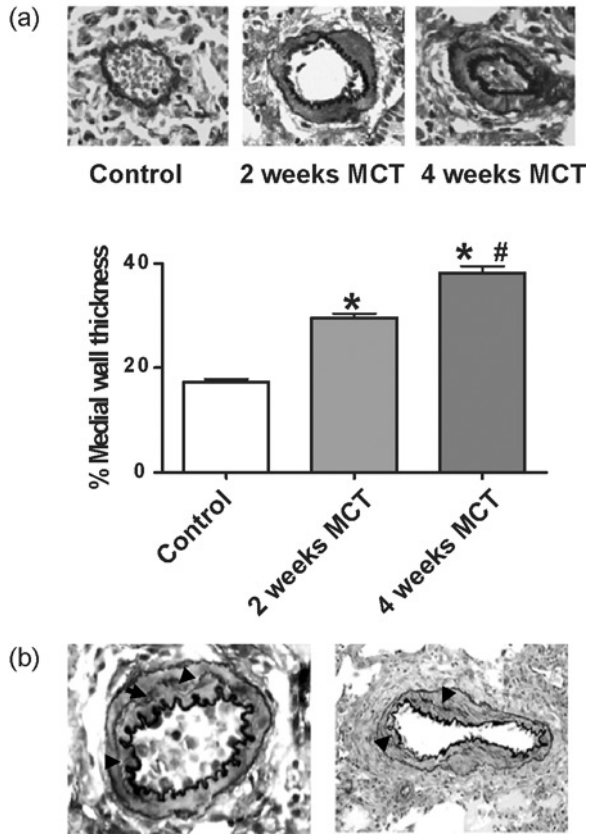

Figure 2 (a) Medial wall hypertrophy. This figure depicts pulmonary arteries from controls, and two and four weeks post-monocrotaline (MCT) rats (size 70–97 μm, magnification $\times$400). There is a significant medial wall thickness in the pulmonary arteries of rats treated with MCT. The bar graph shows progressive medial hypertrophy post-MCT. $^{*}P < 0.05$ versus controls, $^{\#}P < 0.05$ versus two weeks post-MCT ($n = 4$). (b) Fragmentation of elastic laminae in pulmonary arteries. Pulmonary arteries (size 120–160 μm, magnification $\times$200) from two different rats four weeks post-MCT show fragmentation and reduplication of elastic lamina. Black arrows within the medial wall of the arteries point to the fragmented elastic lamina

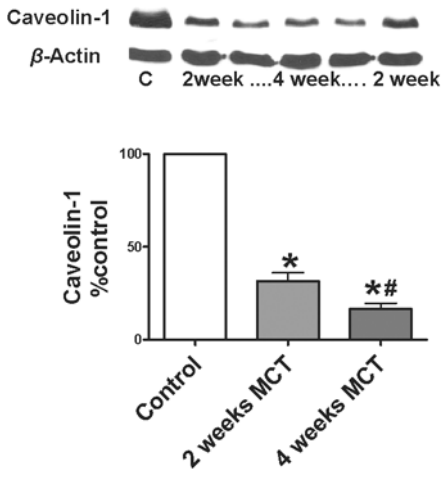

Figure 3 Expression of caveolin-1. A representative Western blot and bar graph showing the expression of caveolin-1 and β-actin in control rat (lane 1), and in rats two weeks post-monocrotaline (MCT) (lanes 2 and 6) and four weeks post-MCT (lanes 3–5). There is a significant and progressive reduction in the expression of caveolin-1 at two to four weeks post-MCT. The expression of β-actin is not altered. $^{*}P < 0.05$ versus controls, $^{\#}P < 0.05$ versus two weeks post-MCT ($n = 7$–9)

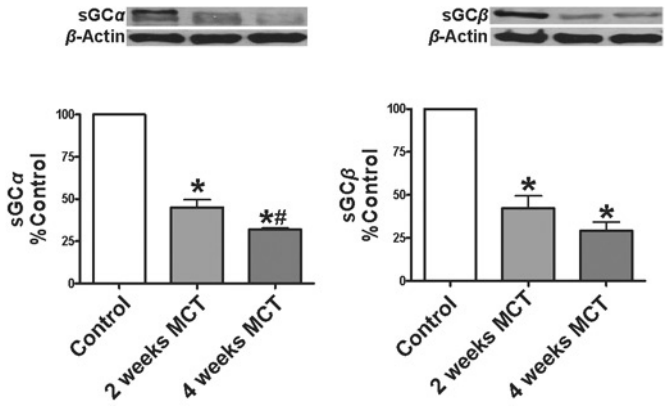

Figure 4 Expression of soluble guanylate cyclase (sGC, α and β subunits). A representative Western blot and bar graph showing the expression of sGC α and β subunits and β-actin in control rat (lane 1), and in rats at two and four weeks post-monocrotaline (MCT) (lanes 2, 3). There is a significant and progressive reduction in the expression of both subunits of sGC at two to four weeks post-MCT. The expression of β-actin is not altered. $^{*}P < 0.05$ versus controls, $^{\#}P < 0.05$ versus two weeks post-MCT ($n = 3$–4)

SDS-polyacrylamide gel (Mini Protean-II; Bio-Rad Laboratories) and transferred to a nitrocellulose membrane (Hybond ECL; Amersham BioSciences, Piscataway, NJ, USA) using Semi Dry Transfer Cell (Bio-Rad Laboratories). The membranes were blocked with 5% non-fat milk powder in Tris-buffered-saline with Tween buffer (TBST, 10 mmol/L Tris-HCl, pH 7.4, 150 mmol/L NaCl, 0.05% Tween 20) at room temperature for one hour. Membranes were then incubated with caveolin-1 (1:5000), PY-STAT3 (1:400), sGC α (1:200), sGC β (1:200), MMP2 (1:200) or Bcl-xL (1:800) overnight at 4°C, according to the manufacturers' recommendations. The membranes were washed for 10 min three times with TBST and incubated with the appropriate secondary antibody for one hour at room temperature, then washed for 10 min three times with TBST buffer. The membranes were reprobed with β-actin (1:8000) or STAT3 (1:2000) to assess protein loading. The protein bands were visualized by chemiluminescence (ECL Western Blotting Analysis System; Amersham Biosciences). The relative expression of the proteins was quantified using densitometric scanning and is expressed as % normal.

Zymography

To assess MMP2 activity, gelatin zymography was performed using a protocol from Bio-Rad with a slight modification. Frozen lung tissues were homogenized in a lysis buffer containing Tris HCl 50 mmol/L (pH 7.6), NaCl 150 mmol/L, $CaCl_2$ 5 mmol/L, 0.05% Brij-35, 0.02% NaN_3 and 1% Triton X-100, and the homogenates centrifuged at 14,000 rpm for 20 min at 4°C. Protein (150 μg) from lung supernatants was loaded on a 8.8% SDS-polyacrylamide gel containing 0.1% gelatin, and run for 70 min at 125V. The gel was washed in 2.5% Triton X-100 for 15 min two times, and incubated overnight at 37°C in a developing buffer containing Tris HCl 50 mmol/L (pH 7.6), $CaCl_2$ 5 mmol/L, NaCl 200 mmol/L and 0.02% Brij-35. The gel was then stained with 0.5% Coomassie Blue G-250 in 10% (v/v) acetic acid and 40% methanol, and left at room temperature for three hours, followed by destaining with a solution containing 10% acetic acid and 40% methanol until clear bands of gelatinolysis appeared on a dark-blue background. Photographs were taken using a digital camera.

Lung histology and morphometric analysis

Formaldehyde-preserved lung tissue was processed for paraffin block; and 5–6 μm sections were cut and stained with elastic van Giesen for evaluation of pulmonary arterial wall thickness. For morphometry, wall thickness and the external diameter of 15–17 arteries (size 45–150 μm) from each rat were measured. Distorted arteries were not used for measurement. Percent medial wall thickness (%WT) was calculated as (2 × wall thickness/external diameter × 100), as described previously.[22]

Double immunofluorescence

Double immunofluorescence was carried out as described previously.[5–7] Briefly, lung sections were mounted on Superfrost plus microscope slides (VWR Scientific, West Chester, PA, USA) in preparation for immunofluorescence. Lung sections were deparaffinized in xylene (5 min two times), rehydrated through a range of aqueous ethyl alcohol solution in H_2O and immersed in PBS for five minutes. Antigen retrieval was performed by incubating the sections in 10 mmol/L citrate buffer, pH 6, in a microwave oven for five minutes. The slides were then incubated in blocking solution (5% normal donkey serum, 0.5% Triton in PBS) for one hour at room temperature, followed by an overnight incubation at 4°C with the primary antibody (caveolin-1α, 1:100) or MMP2 (polyclonal antibody from Sigma, 1:50) in blocking solution. The next day, the slides were washed with PBS for 10 min three times and incubated

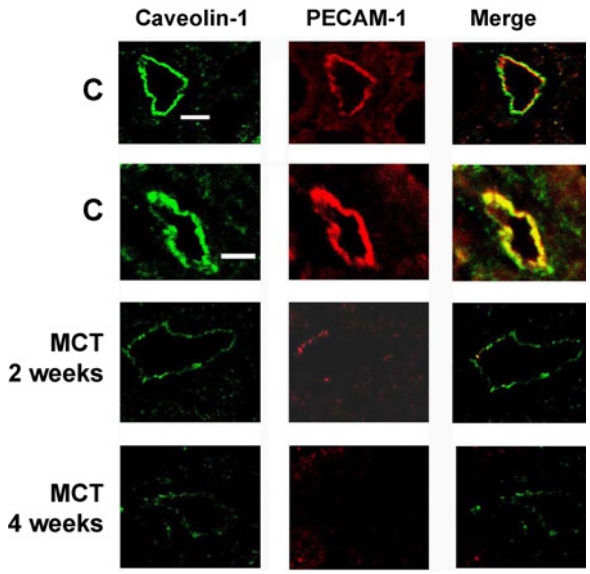

Figure 5 Expression of caveolin-1 and PECAM-1. Immunofluorescence study depicting the expression of caveolin-1 (green) and PECAM-1 (red) in pulmonary arteries from two controls and two and four weeks post-monocrotaline (MCT). PECAM-1 colocalizes with caveolin-1 and both caveolin-1 and PECAM-1 are lost at two and four weeks post-MCT. Bar = 50μm

in Alexa 488 (donkey anti-rabbit, 1:300, green color; Molecular Probes, Eugene, OR, USA) at room temperature in a dark place for one hour followed by washing in PBS for 10 min three times. For double staining, the sections were blocked again, as described earlier, and incubated in the primary antibodies PECAM-1 (1:50), vWF (1:50) or smooth muscle α-actin (1:15) overnight; the procedure was repeated using the secondary antibody (Alexa 594, donkey anti-rabbit 1:200, or anti-goat 1:200, red color; Molecular Probes). The sections were examined with a laser scanning confocal fluorescence microscope (MRC 1000; Bio-Rad). The negative controls were run in the absence of primary antibodies.

Statistical analysis

The data are expressed as means $\pm$ SE. For statistical analysis, we used one way analysis of variance followed by Scheffe's multiple comparison tests. Differences were considered statistically significant at $P < 0.05$. From caveolin-1/smooth muscle α-actin double immunofluorescence studies, the percentage of arteries showing endothelial caveolin-1 and enhanced expression of caveolin-1 in SMC ($n = 3$–5), and from caveolin-1/vWF immunofluorescence studies, the arteries exhibiting vWF loss and the enhanced expression of caveolin-1 in SMC ($n = 5$–6), were calculated. In addition, the size range of arteries exhibiting enhanced expression of caveolin-1 in SMC at four weeks post-MCT was analyzed ($n = 4$).

Results

Weight gain in MCT-treated rats

The weight gain at two weeks post-MCT was lower compared with the controls ($38 \pm 3\%$ versus $67 \pm 9\%$, $P < 0.05$). At four weeks post-MCT, rats actually lost weight ($17 \pm 4\%$) and several rats showed signs of congestive heart failure such as ascites and pleural effusion. The mortality rate in this group was 38%. There were no deaths at two weeks post-MCT.

MCT induces progressive PH, RVH and vascular remodeling

As shown in Figure 1, there was a significant increase in RVSP indicative of PH, and RVH at two weeks post-MCT with a further increase in RVSP and RVH at four weeks. Consistent with the hemodynamic data, the pulmonary arteries showed progressively increasing medial wall thickness at two and four weeks post-MCT. This observation was further confirmed by morphometric analysis (Figure 2a). Fragmentation of the elastic laminae was observed in pulmonary arteries (size $>120\,\mu$m, Figure 2b) at four weeks post-MCT. At two weeks post-MCT, fragmentation of elastic laminae was not evident. We have previously shown at three weeks post-MCT, fragmentation of elastic laminae indicative of elastolytic activity in the main and in larger resistant arteries (size $>300\,\mu$m).[7,23] Thus, as the disease progresses, smaller arteries begin to exhibit fragmentation of elastic laminae.

MCT induces progressive loss of endothelial cell membrane proteins

Western blot analysis (expression of caveolin-1 and sGC subunits, α and β)

Western blot analysis in Figure 3 depicts significant and progressive loss of caveolin-1 at two and four weeks post-MCT compared with the controls. The expression of β-actin, used to assess the protein loading, was not altered. Both subunits of sGC proteins show significant and progressive loss in the lungs from rats at two and four weeks post-MCT similar to caveolin-1 loss (Figure 4). This is consistent with our previous observation; and sGC has been shown to co-localize with caveolin-1 in endothelial caveolae to facilitate NO activity.[7,24]

Localization of caveolin-1 and PECAM-1

Next, we conducted a double immunofluorescence study to localize the expression of caveolin-1 and PECAM-1, another membrane protein. Both PECAM-1 and endothelial caveolin-1 co-localize, and are lost at two and four weeks post-MCT (Figure 5). We have previously shown that the loss of PECAM-1 occurs in tandem with caveolin-1 as early as 48 h post-MCT.[6] These results indicate a generalized disruption of endothelial cell membrane in the MCT model, and the progressive nature of EC damage.

Activation of cell proliferative and anti-apoptotic pathways

There is a significant increase in the activation of PY-STAT3 at two weeks post-MCT with a further increase at four weeks (Figure 6a). Similarly, increased expression of

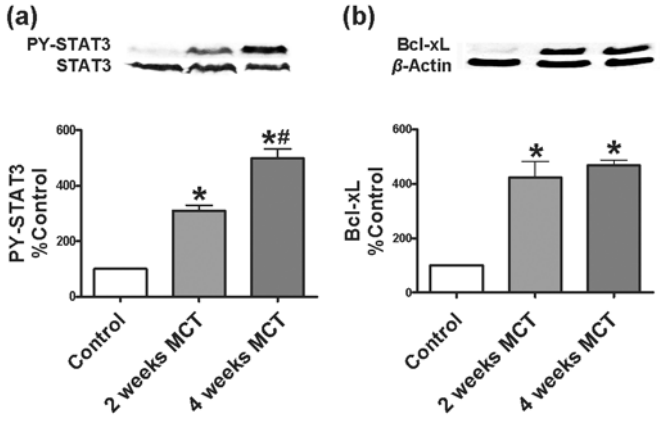

Figure 6 Activation of PY-STAT3 and upregulation of Bcl-xL. (a) Representative Western blot and bar graph showing the expression of PY-STAT3 and STAT3 in control rats (lane 1), and in rats at two and four weeks post-MCT (lanes 2, 3). There is a significant and progressive increase in the activation of PY-STAT3 at two to four weeks post-MCT. The expression of STAT3 is not altered ($n = 4–5$). (b) Representative Western blot and bar graph showing the expression of Bcl-xL and β-actin in control rats (lane 1), and in rats at two and four weeks post-MCT (lanes 2, 3). There is a significant increase in the expression of Bcl-xL at two to four weeks post-monocrotaline (MCT). The expression of β-actin is not altered. $^{*}P < 0.05$ versus controls, $^{\#}P < 0.05$ versus two weeks post-MCT ($n = 4$)

Bcl-xL is found at two and four weeks post-MCT (Figure 6b). The activation of PY-STAT3 and increased expression of Bcl-xL have been shown to occur as early as within 48 h of MCT injection, in parallel with endothelial caveolin-1 loss, before the onset of PH. Importantly, rescue of endothelial caveolin-1 abrogates the activation of proliferative pathways and attenuates PH.[8,25,26] Thus, the loss of inhibitory function of caveolin-1 results in the activation of proliferative pathways leading to vascular remodeling and PH. These results underscore the protective function of endothelial caveolin-1 in pulmonary vasculature.

Loss of vWF is associated with an enhanced expression of caveolin-1 in SMC

Expression of caveolin-1 and smooth muscle α-actin

The expression and localization of caveolin-1 and smooth muscle α-actin are presented in Figure 7. Progressive loss of endothelial caveolin-1 is seen at two and four weeks post-MCT (Figure 7a). In controls, there was no loss of endothelial caveolin-1. At two weeks post-MCT, the number of arteries exhibiting endothelial caveolin-1 was significantly reduced ($26 \pm 2.7\%$ versus control 100%, $P < 0.05$), with a further reduction at four weeks ($15 \pm 1.8\%$, $P < 0.05$ versus two weeks post-MCT). At two weeks post-MCT, however, there was no evidence of enhanced expression of caveolin-1 in SMC. At four weeks post-MCT, there was not only a further loss of endothelial caveolin-1, but also $23 \pm 1.8\%$ of arteries exhibited enhanced expression of caveolin-1 in SMC (Figure 7b). Importantly, an enhanced expression of caveolin-1 in SMC was seen mainly in smaller arteries (range 20–203 μm); 80% of arteries were <100 μm in size (71% in <75 μm), 13% in the 100–150 μm range and 7% in >150 μm. Despite the enhanced expression of caveolin-1 in SMC, the protein as assessed by Western blot analysis, showed significant reduction in the total amount of caveolin-1 at four weeks post-MCT (Figure 3). The possible reasons are that at four weeks post-MCT (a) there is a significant loss in the expression of endothelial caveolin-1; importantly, endothelial cells have a much higher amount of caveolin-1 as compared with SMC[27] and (b) because vascular disease does not progress uniformly in PH. Loss of endothelial caveolin-1 occurs in 85% of arteries and the enhanced expression of caveolin-1 is present in $\sim$23% of the arteries. As the diseases progresses further, it is likely that more arteries will exhibit enhanced expression of caveolin-1 in SMC. These data do show the sequence of alterations in caveolin-1 expression during the progression of PH.

Expression of caveolin-1 and vWF

To further investigate the enhanced expression of caveolin-1 in SMC, we conducted a double immunofluorescence study using caveolin-1 and vWF antibodies. Double immunofluorescence revealed progressive loss of endothelial caveolin-1 at two and four weeks post-MCT, but the expression of vWF was well preserved at two weeks, consistent with our previous studies.[6] Furthermore, there was no evidence of enhanced expression of caveolin-1 in SMC (Figure 8a). However, at four weeks post-MCT, $29 \pm 2.7\%$ arteries exhibited vWF loss and 70% of these arteries revealed enhanced expression of caveolin-1 in SMC. Importantly, enhanced expression of caveolin-1 in SMC was observed only in arteries which exhibited the loss of vWF (Figure 8b). Since vWF is found in Weibel Palade bodies within the endothelial cells, its loss is indicative of extensive EC damage or loss, and the enhanced expression of caveolin-1 in SMC follows the extensive endothelial damage.

Increased expression and activation of MMP 2

As depicted in Figure 9a, there is a significant increase in the expression of MMP2 at two-weeks post-MCT and a further increase at four weeks post-MCT. The zymogram in Figure 9b shows progressively increased expression of proMMP2 and activity of MMP2 in the two and four weeks post-MCT groups. Although Western blot and zymogram revealed increased expression of MMP2 at two weeks post-MCT, immunofluorescence studies revealed MMP2 expression in SMC only at four weeks post-MCT (Figure 9c). Since caveolin-1 co-localizes with MMP2 and keeps proteolysis of matrix under control, it is likely that the increased expression and activity of MMP2 at two weeks post-MCT is the result of endothelial caveolin-1 loss. At four weeks post-MCT, further loss of endothelial caveolin-1 and translocation of caveolin-1 from caveolae in SMC may be responsible for further increased expression and activity of MMP2. Thus, increased expression and activity of MMP2 coupled with enhanced expression of caveolin-1 in SMC may facilitate cell proliferation and cell migration, and perhaps eventually lead to neointima formation.

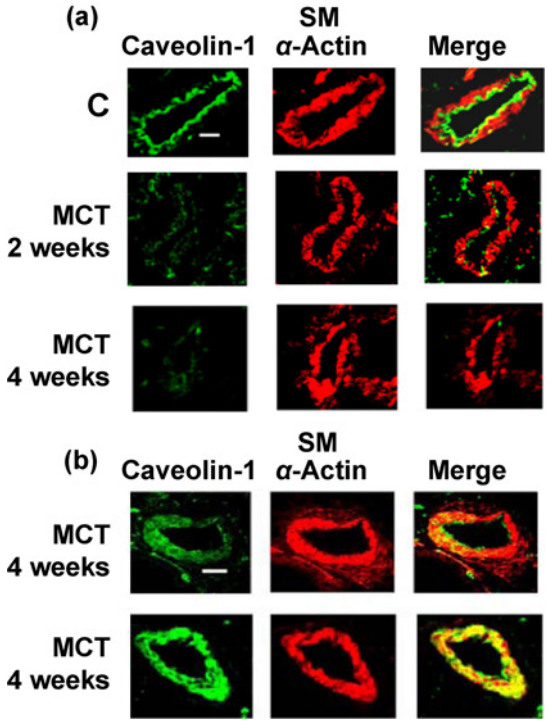

Figure 7 Expression of caveolin-1 and smooth muscle α-actin. Immunofluorescence study depicting the expression of caveolin-1 (green) and smooth muscle α-actin (red) in pulmonary arteries from control and at two and four weeks post-monocrotaline (MCT). (a) There is progressive loss of endothelial caveolin-1. (b) This figure depicts loss of endothelial caveolin-1 in two arteries at four weeks post-MCT accompanied by enhanced expression of caveolin-1 in smooth muscle cells. Bar = 50μm

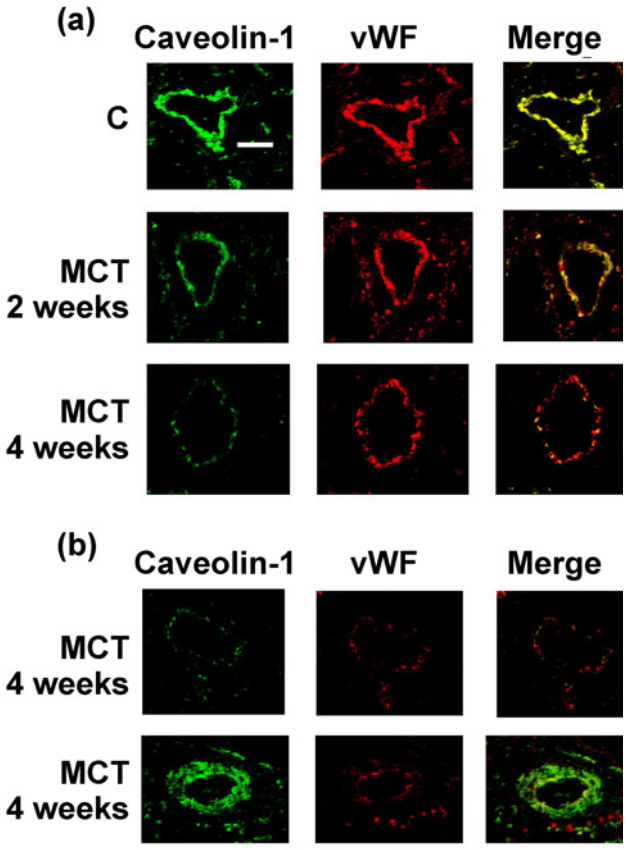

Figure 8 Expression of caveolin-1 and von Willebrand factor (vWF). Immunofluorescence study depicting the expression of caveolin-1 (green) and vWF (red) in pulmonary arteries from control and two and four weeks post-monocrotaline (MCT). (a) There is progressive loss of endothelial caveolin-1. The expression of vWF is well preserved at two weeks post-MCT, and at four weeks, reduction in the expression of vWF can be seen. (b) At four weeks post-MCT, arteries with vWF loss exhibit enhanced expression of caveolin-1 in smooth muscle cells. Bar = 50μm

Discussion

The main findings of this study are: (1) a single subcutaneous injection of MCT is associated with a progressive loss of endothelial caveolin-1, activation of PY-STAT3, increased expression of Bcl-xL, vascular remodeling and PH at two and four weeks post-MCT; (2) the expression of PECAM-1 and sGC (α and β subunits) known to localize in the endothelial caveolae is lost concomitantly with endothelial caveolin-1; (3) despite the presence of a significant PH at two weeks post-MCT, the expression of vWF is well preserved and there is no evidence of enhanced expression of caveolin-1 in SMC; (4) at four weeks post-MCT, with a further loss of endothelial caveolin-1, several arteries ($29 \pm 2.7\%$) begin to show a loss of vWF; and (5) the enhanced expression of caveolin-1 in SMC is seen in 70% of the arteries exhibiting the loss of vWF; (6) a seven-fold increase in the expression of MMP2 was observed at four weeks post-MCT and three-fold at two weeks. These studies suggest that the loss of endothelial caveolin-1 associated with the activation of proliferative and antiapoptotic pathways initiates the disease process leading to PH and RVH. As the disease progresses, the resulting extensive endothelial damage/loss as evidenced by vWF loss, leads to the enhanced expression of caveolin-1 in SMC, and the associated increased expression and activity of MMP2 may further facilitate cell proliferation and cell migration, and possibly participate in neointima formation.

STAT3 is a member of the STAT family of latent transcription factors, activated by phosphorylation. PY-STAT3 is translocated to nuclei and activates genes involved in cell proliferation and antiapoptosis. Some of the key downstream mediators of PY-STAT3 are Bcl-xL, cyclin D1 and survivin, all of which have been implicated in PH.[7,26,28] PY-STAT3 is a downstream effector of the proinflammatory cytokine, interleukin-6 (IL-6). Inflammation has an important role in human and experimental forms of PH.[29] MCT-induced PH is associated with progressive upregulation of IL-6 mRNA, increased IL-6 bioactivity and increased expression of glycoprotein (gp) 130, a shared receptor of IL-6; IL-6/gp130 signaling activates PY-STAT3. In the MCT model of PH, the loss of endothelial caveolin-1 associated with the activation of proliferative (PY-STAT3) and antiapoptotic (Bcl-xL) pathways occurs before the onset of PH.[6,7] Interestingly, caveolin-1 inhibits the activation of PY-STAT3, and the activated PY-STAT3 can inhibit the transcription of caveolin-1 by binding to its promoter.[30,31]

Initial loss of endothelial caveolin-1, accompanied by the loss of other membrane proteins, is indicative of generalized disruption of endothelial cell membrane integrity. This is followed by the loss of several cytosolic proteins, suggesting

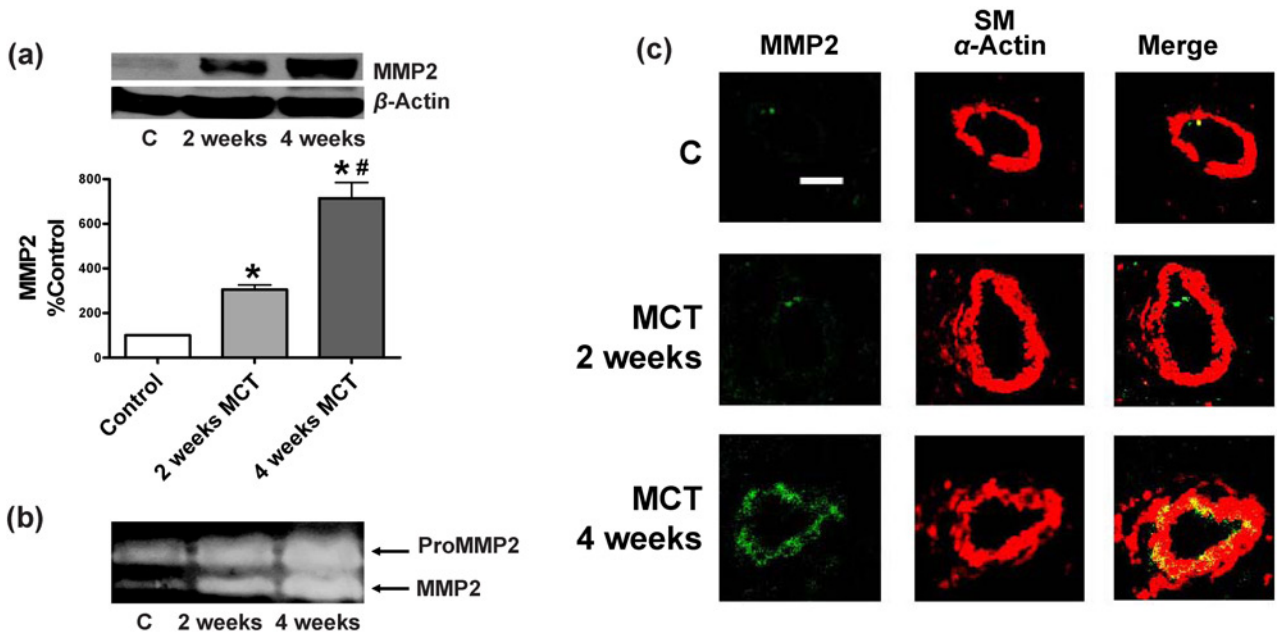

Figure 9 Expression of matrix metalloproteinase 2 (MMP2). A representative Western blot and bar graph showing the expression of MMP2 and β-actin in control rat (lane 1), and in rats two and four weeks post-monocrotaline (MCT) (lanes 2, 3). There is a significant and progressive increase in the expression of MMP2 at two to four weeks post-MCT. The expression of β-actin is not altered. $^{*}P < 0.05$ versus controls, $^{\#}P < 0.05$ versus two weeks post-MCT ($n = 5$–6, a). (b) Zymograph showing increased expression of proMMP2 and the active form of MMP2 at two weeks post-MCT and a further increase at four weeks post-MCT. Immunofluorescence study (c) depicting the expression of MMP2 (green) and smooth muscle α-actin (red) in pulmonary arteries from control and at two and four weeks post-MCT. MMP2 was not expressed in the controls or at two weeks post-MCT. AT four weeks post-MCT, a few pulmonary arteries exhibited the expression of MMP2 in the smooth muscle cells. Bar = 50μm. MMP2, matrix metalloproteinase 2

progressive endothelial cell damage.[7] What is important in the present study is that as the disease progresses, pulmonary arteries at four weeks post-MCT begin to exhibit the loss of vWF in addition to the extensive loss of endothelial caveolin-1. Significantly, enhanced expression of caveolin-1 in SMC appears only in the arteries exhibiting the loss of vWF. vWF is a large adhesive glycoprotein, synthesized by vascular endothelial cells and stored in Weibel Palade bodies.[32] An increased plasma level of vWF is considered to be a marker for endothelial cell damage, and an elevated level of vWF is a predictor of poor outcome in patients with idiopathic PAH.[17,33,34] Recently, it was reported that circulating angiopoietin-2 correlated with the severity of the disease in patients with idiopathic PAH.[35] It is important to note that angiopoietin-2 is also stored in Weibel Palade bodies. As the endothelial disruption progresses, Weibel Palade bodies lose their cargo, possibly as a result of ensuing extensive endothelial damage or loss. Furthermore, increased levels of circulating endothelial cells are seen in patients with irreversible PH.[18] Thus, the extensive damage or loss of EC facilitates irreversibility of PH. Our studies show that the initial loss of endothelial caveolin-1 is progressive, resulting in extensive endothelial damage as evidenced by vWF loss, followed by enhanced expression of caveolin-1 in SMC, which may lead to further cell proliferation and migration, and ultimately to neointima formation.

Vascular SMC play an important role in the pathobiology of PH. During the progression of PH, SMC change from a contractile to a synthetic phenotype. These cells then can proliferate and migrate, leading to neointima formation. The underlying mechanism of SMC phenotype transformation and their migration has not been fully defined. Juxtaposition of EC and SMC facilitates crosstalk and co-regulation. EC protect underlying SMC from elements of blood and direct pressure and shear stress, and inhibit growth and proliferation, thus, keeping SMC in a quiescent state. Caveolin-1 functions as an antiproliferative factor also in SMC; it keeps mitogens inactive and regulates Ca^{2+} entry in SMC. Furthermore, caveolin-$1^{-/-}$ SMC exhibit propensity to proliferate and migrate.[36,37] PDGF receptors have been implicated in vascular SMC proliferation and migration. Increased expression of PDGF receptor in experimental and human PH has recently been reported, and the inhibition of PDGF receptor resulted in significant amelioration of experimental PH.[38] Interestingly, caveolin-1 co-localizes with PDGF receptors and prevents their auto-phosphorylation.[39] It is worth noting that the loss or dysfunction of endothelial caveolin-1 is an important feature in experimental models of PH and human PH.[5,13,19]

Under normal conditions, caveolin-1 keeps ERK inactive in caveolae. In response to cyclic strain, in cultured SMC, caveolin-1 translocates from caveolae to non-caveolar sites within the plasma membrane, and the translocated caveolin-1 mediates ERK activation, thus, facilitating cell cycle progression and cell proliferation. Caveolin-1 antisense treatment abolishes the stretch-induced cell proliferation, indicating that caveolin-1 may play a pivotal role in stretch-induced cell proliferation.[40,41] Thus, the extensive damage and/or loss of endothelial cells observed in PH may impose wall strain induced by elevated pressure directly on to SMC, leading to translocation of caveolin-1

from caveolae and increased expression in SMC. It is worth noting that at four weeks post-MCT, extensive damage/loss of endothelial cells with enhanced expression of caveolin-1 in SMC is associated with much higher pulmonary artery pressure (in mmHg, control, 19 ± 0.5; 2 weeks, $35 \pm 2^{*}$; 4 weeks, $45 \pm 3^{*\#}$; $^{*}P < 0.05$ versus control, $^{\#}P < 0.05$ versus 2 weeks). Thus, at four weeks post-MCT, in the presence of extensive endothelial damage and/or loss, SMC are directly exposed to the higher pressure, which may be responsible for translocation of caveolin-1 from caveolae to non-caveolar sites, and its increased expression in SMC. This translocation of caveolin-1 results in the loss of its ability to inhibit the proliferative molecules that reside in caveolae, which facilitates further cell proliferation and cell migration. Significantly, SMC isolated from patients with PAH reveal enhanced caveolin-1 expression, altered Ca^{2+} handling, increased capacitative Ca^{2+} entry, increased $[Ca^{2+}]_i$ and DNA synthesis. Silencing caveolin-1 mRNA in these SMC has inhibitory effect on capacitance Ca^{2+} entry and DNA synthesis.[19] These results strongly suggest that the enhanced expression of caveolin-1 in SMC and possible translocation to non-caveolar sites during the progression of pulmonary vascular disease mishandles Ca^{2+} regulation, and not only does it lose its capacity to inhibit cell proliferation, but also actively participates in cell proliferation and perhaps contributes to neointima formation.

MMP2 belongs to a gelatinase subgroup of a family of zinc-containing proteolytic enzymes with different substrate specificities responsible for the breakdown of extracellular matrix. Vascular SMC in culture have been shown to synthesize and secrete the active form of MMP2, capable of degrading extracellular matrix barrier. Activation of MMP2 is associated with increased SMC proliferation and migration. Reported increased MMP2 activity in cultured SMC from patients with idiopathic PAH[20] may, in part, be responsible for matrix degradation, cell migration and eventual neointima formation. Interestingly, in a carotid flow cessation model, MMP2-deficient mice developed significantly less intimal proliferation compared with the wild-type mice;[42] and furthermore, MMP2 inhibitor has been shown to induce regression of vascular remodeling in the pulmonary artery explants from rats three weeks post-MCT.[43] Fragmentation of elastic laminae has been observed at three and four weeks post-MCT,[7,23] and in the present study. Interestingly, elastin can act as a template for proMMP2 and its activation to induce its own proteolysis.[44] In the present study, the expression and activity of MMP2 progressively increased from two to four weeks post-MCT. The immunofluorescence study, however, revealed MMP2 expression in SMC only at four weeks post-MCT, but not at two weeks.

Membrane type 1-matrix metalloproteinase (MT1-MMP), a physiological activator of proMMP2, is preferentially localized in caveolae. Caveolin-1 negatively regulates MT1-MMP and MMP2 activity, thus inhibiting cell migration.[21,45–47] Increased expression of MMP2 in SMC at four weeks post-MCT, despite the presence of enhanced expression of caveolin-1, suggests that caveolin-1 may not be in caveolae, thus, has lost its inhibitory effect on signaling molecules residing in caveolae. Further studies are required to examine the precise mechanism/s of enhanced expression of caveolin-1 in SMC and increased MMP2 expression during the progression of PH. Thus, in PH, the switch from an antiproliferative to proproliferative function may depend on alteration in caveolin-1 conformation, localization, cell context and the stage of the disease.[13]

In conclusion, MCT-induced progressive loss of endothelial caveolin-1 is associated with the activation of cell proliferative and anti-apoptotic pathways, leading to vascular remodeling and PH by two weeks. As the endothelial cell damage progresses, by four weeks post-MCT, the loss of vWF, indicative of extensive EC damage or loss, is accompanied by enhanced expression of caveolin-1 in SMC. Thus, the enhanced expression of caveolin-1 in SMC is a sequential event in the progression of PH, occurring after the extensive EC damage or loss, which may foreshadow SMC phenotype change, further cell proliferation, cell migration and neointima formation. Thus, the modulation of caveolin-1 may be of therapeutic value in the management of PH.

Author contributions: All authors participated in the design and discussion of the experiments. JH conducted the animal experiments, Western blot analysis and immunofluorescence, and assisted in collecting data. JHW helped with paraffin blocks and slide preparation and interpreted the lung pathology. RM interpreted the data and wrote the manuscript. JH, JHW and MHG read the manuscript and approved it.

ACKNOWLEDGEMENTS

The study was supported, in part, by a grant from Maria Fareri Children's Hospital Research Fund (to RM).

REFERENCES

1 Simonneau G, Robbins IM, Beghetti M, Channick RN, Delcroix M, Denton CP, Elliott CG, Gaine SP, Galdwin MT, Jing ZC, Krowka MJ, Langleben D, Nakanishi N, Souza R. Updated clinical classification of pulmonary hypertension. *J Am Coll Cardiol* 2009;**54**:S43–54
2 Badesch DB, Raskob GE, Elliott G, Krichman AM, Farber HW, Frost AE, Barst RJ, Benza RL, Liou TG, Turner M, Giles S, Feldkircher K, Miller DP, McGoon MD. Pulmonary arterial hypertension. Baseline characteristics from the REVEAL registry. *Chest* 2010;**137**:376–87
3 Selimovic N, Bergh CH, Andersson B, Sakiniens E, Carlsten H, Rundquist B. Growth factors and interleukin-6 across the lung circulation in pulmonary hypertension. *Eur Respir J* 2009;**34**:662–8
4 Mathew R, Zeballos G, Tun H, Gewitz MH. Role of nitric oxide and endothelin 1 imbalance in monocrotaline-induced pulmonary hypertension in rats. *Cardiovasc Res* 1995;**30**:739–46
5 Mathew R, Huang J, Katta UD, Krishnan U, Sandoval C, Gewitz MH. Immunosuppressant-induced endothelial damage and pulmonary arterial hypertension. *J Ped Hem Onc* 2011;**33**:55–8
6 Mathew R, Huang J, Shah M, Patel K, Gewitz MH, Sehgal PB. Disruption of endothelial-cell caveolin-1 alpha/raft scaffolding during the development of monocrotaline-induced pulmonary hypertension. *Circulation* 2004;**110**:1499–506
7 Huang J, Wolk JH, Gewitz MH, Mathew R. Progressive endothelial cell damage in an inflammatory model of pulmonary hypertension. *Expt Lung Res* 2010;**36**:57–66
8 Huang J, Kaminski PM, Edwards JG, Yeh A, Wolin MS, Frishman WH, Gewitz MH, Mathew R. Pyrrolidine dithiocarbamate restores endothelial

cell membrane integrity and attenuates monocrotaline-induced pulmonary artery hypertension. *Am J Physiol* 2008;**294**:L1250–L1259
9 Mathew R, Yuan N, Rosenfeld L, Gewitz MH, Kumar A. Effects of monocrotaline on eNOS expression and sulfhydryl levels in rat lungs heart disease 2002;**4**:152–8
10 Liu P, Rudick M, Anderson RGW. Multiple functions of caveolin-1. *J Biol Chem* 2002;**277**:41295–8
11 Couet J, Li S, Okamoto T, Ikezu T, Lisanti MP. Identification of peptide and protein ligand for the caveolin-1 scaffolding domain. Implications for the interaction of caveolin and caveolae associated proteins. *J Biol Chem* 1997;**272**:6535–3
12 Okamoto T, Schlegel A, Scherer PE, Lisanti MP. Caveolins, a family of scaffolding proteins for organizing pre-assembled signaling complexes at the plasma membrane. *J Biol Chem* 1998;**273**:5419–22
13 Mathew R. Cell-specific dual role of caveolin-1 in pulmonary hypertension. *Pulm Med* 2011;**2011**:573432
14 Galbiati F, Volonté D, Liu J, Capazzo F, Frank PG, Zhu L, Pestell RG, Lisanti MP. Caveolin-1 expression negatively regulates cell cycle progression by inducing G(0)/G(1) arrest via a p53/p21(WAF1/Cip1)-dependent mechanism. *Mol Biol Cell* 2001;**12**:2229–44
15 Torres VA, Tapia JC, Rodríguez DA, Párraga M, Lisboa P, Montoya M, Leyton L, Quest AF. Caveolin-1 controls cell proliferation and cell death by suppressing expression of the inhibitor of apoptosis protein survivin. *J Cell Sci* 2006;**119**:1812–23
16 Hardin CD, Vallejo J. Caveolins in vascular smooth muscle: form organizing function. *Cardiovasc Res* 2006;**69**:808–15
17 Kawut SM, Horn EM, Berekashvili KK, Widlitz AC, Rosenzweig EB, Barst RJ. Von Willebrand factor independently predicts long-term survival in patients with pulmonary arterial hypertension. *Chest* 2005;**128**:2355–62
18 Smadja DM, Gaussem P, Mauge L, Israël-Biet D, Dignat-George F, Peyrard S, Agnoletti G, Vouhé PR, Bonnet D, Lévy M. Circulating endothelial cells: a new candidate biomarker of irreversible pulmonary hypertension secondary to congenital heart disease. *Circulation* 2009;**119**:374–81
19 Patel HH, Zhang S, Murray F, Suda RY, Head BP, Yokoyama U, Swaney JS, Niesman IR, Schermuly RT, Pullamsetti SS, Thistlethwaite PA, Miyanohara A, Farquhar MG, Yuan JX, Insel PA. Increased smooth muscle cell expression of caveolin-1 and caveolae contribute to the pathophysiology of idiopathic pulmonary arterial hypertension. *FASEB J* 2007;**21**:2970–9
20 Lepetit H, Eddahibi S, Fadel E, Frisdal E, Munaut C, Noel A, Humbert M, Adnot S, D'Ortho MP, Lafuma C. Smooth muscle cell matrix metalloproteinases in idiopathic pulmonary arterial hypertension. *Eur Respir J* 2005;**25**:834–42
21 Chow AK, Cena J, El-Yazbi AF, Crawford BD, Holt A, Cho WJ, Daniel EE, Schulz R. Caveolin-1 inhibits matrix metalloproteinase-2 activity in the heart. *J Mol Cell Cardiol* 2007;**42**:896–901
22 Mathew R, Gloster ES, Sundararajan T, Thompson CI, Zeballos G, Gewitz MH. Role of inhibition of nitric oxide production in monocrotaline-induced pulmonary hypertension. *J Appl Physiol* 1997;**82**:1493–8
23 Mathew R, Guzowski DE, Gloster ES. Effect of verapamil on monocrotaline-induced pulmonary artery hypertension and endothelial cell dysfunction in rats. *Exp Lung Res* 1990;**16**:627–44
24 Linder AE, McCluskey LP, Cole KR 3rd, Lanning KM, Webb RC. Dynamic association of nitric oxide downstream signaling molecules with endothelial caveolin-1 in rat aorta. *J Pharmacol Exp Ther* 2005;**314**:9–15
25 Mathew R, Huang J, Gewitz MH. Pulmonary artery hypertension: caveolin-1 and eNOS interrelationship: a new perspective. *Cardiol Rev* 2007;**15**:143–9
26 Jasmin JF, Mercier I, Dupuis J, Tanowitz HB, Lisanti MP. Short-term administration of a cell-permeable caveolin-1 peptide prevents the development of monocrotaline-induced pulmonary hypertension and right ventricular hypertrophy. *Circulation* 2006;**114**:912–20
27 Frank PG, Woodman SE, Park DS, Lisant MP. Caveolin, caveolae, and endothelial cell function. *Arterioscler Thromb Vasc Biol* 2003;**23**:1161–8
28 McMurtry MS, Archer SL, Altieri DC, Bonnet S, Haromy A, Harry G, Bonnet S, Puttagunta L, Michelakis ED. Gene therapy targeting survivin selectively induces pulmonary vascular apoptosis and reverses pulmonary arterial hypertension. *J Clin Invest* 2005;**115**:1479–91
29 Mathew R. Inflammation and pulmonary hypertension. *Cardiol Rev* 2010;**18**:67–72.
30 Jasmin JF, Mercier I, Sotgia F, Lisanti MP. SOCS proteins and caveolin-1 as negative regulators of endocrine signaling. *Trends Endocrinol Metab* 2006;**17**:150–8
31 Chiu WT, Lee HT, Huang FJ, Aldape KD, Yao J, Steeg PS, Chou CY, Lu Z, Xie K, Huang S. Caveolin-1 upregulation mediates suppression of primary breast tumor growth and brain metastases by Stat3 inhibition. *Cancer Res* 2011;**71**:4932–43
32 Ewenstein BM, Warhol MJ, Handin RI, Pober JS. Composition of the von Willebrand factor storage organelle (Weibel Palade body) isolated from cultured human umbilical vein endothelial cells. *J Cell Biol* 1987;**104**:1423–33
33 Collados MT, Sandoval J, Lopez S, Massó FA, Páez A, Borbolla JR, Montaño LF. Characterization of von Willebrand factor in primary pulmonary hypertension. *Heart Vessels* 1999;**14**:246–52
34 Lip GY, Blann A. von Willebrand factor: a marker of endothelial dysfunction in vascular disorders? *Cardiovasc Res* 1997;**34**:255–65
35 Kümpers P, Nickel N, Lukasz A, Golpon H, Westerkamp V, Olsson KM, Jonigk d, Maegel L, Bockmeyer CL, Dacid S, Hoeper MM. Circulating angiopoietins in idiopathic pulmonary arterial hypertension. *Eur Heart J* 2010;**31**:2291–30
36 Hassan GS, Williams TM, Frank PG, Lisanti MP. Caveolin-1-deficient aortic smooth muscle cells show cell autonomous abnormalities in proliferation, migration, and endothelin-based signal transduction. *Am J Physiol* 2006;**290**:H2393–H2401
37 Isshiki M, Anderson RG. Function of caveolae in Ca2+ entry and Ca2+-dependent signal transduction. *Traffic* 2003;**4**:717–23
38 Schermuly RT, Dony E, Ghofrani HA, Pullamsetti S, Savai R, Roth R, Sydkov A, Lai YJ, Weissmann N, Seeger W, Grimminger F. Reversal of experimental pulmonary hypertension by PDGF inhibition. *J Clin Invest* 2005;**115**:2811–21
39 Yamamoto M, Toya Y, Jensen RA, Ishikawa Y. Caveolin-1 is an inhibitor of platelet-derived growth factor receptor signaling. *Expt Cell Res* 1999;**247**:380–8
40 Kawabe J, Okumura S, Lee MC, Sadoshima J, Ishikawa Y. Translocation of caveolin regulates stretch-induced ERK activity in vascular smooth muscle cells. *Am J Physiol* 2004;**286**:H1845–H1852
41 Sedding DG, Braun-Dullaeus RC. Caveolin-1: dual role for proliferation of vascular smooth muscle cells. *Trends Cardiovasc Med* 2006;**16**:50–5
42 Kuzuya M, Kanda S, Sasaki T, Tamaya-Mori N, Cheng XW, Itoh T, Itohara S, Iguchi A. Deficiency of gelatinase A suppresses smooth muscle invasion and development of experimental intimal hyperplasia. *Circulation* 2003;**108**:1375–81
43 Cowan KN, Jones PL, Rabinovitch M. Elastase and matrix metalloproteinase inhibitors induce regression, and tenascin-C antisense prevents progression, of vascular disease. *J Clin Invest* 2000;**105**:21–34
44 Emonard H, Hornebeck W. Binding of 92 kDa and 72 kDa progelatinases to insoluble elastin modulates their proteolytic activation. *Biol Chem* 1997;**378**:265–71
45 Annabi B, Lachambre M, Bousquet-Gagnon N, Pagé M, Gingras D, Béliveau R. Localization of membrane type 1 metalloproteinase in caveolae membrane domains. *Biochem J* 2001;**353**:547–53
46 Newby AC. Matrix metalloproteinases regulate migration, proliferation, and death of vascular smooth muscle cells by degrading matrix and non-matrix substrates. *Cardiovasc Res* 2006;**69**:614–24
47 Pauly RR, Passanti A, Bilato C, Monticone R, Cheng L, Papadopoulos N, Gluzband YA, Smith L, Weinstein C, Lakatta EG. Migration of cultured vascular smooth muscle cells through a basement membrane barrier requires type IV collagenase activity and is inhibited by cellular differentiation. *Circ Res* 1994;**75**:41–54

(Received November 9, 2011, Accepted May 14, 2012)